BEX1 is differentially expressed in aldosterone-producing adenomas and protects human adrenocortical cells from ferroptosis

Yuhong Yang[1], Martina Tetti[2], Twinkle Vohra[1], Christian Adolf[1], Jochen Seissler[3], Michael Hristov[4], Alexia Belavgeni[5], Martin Bidlingmaier[1], Andreas Linkermann[5], Paolo Mulatero[2], Felix Beuschlein[1,6,] Martin Reincke[1], Tracy Ann Williams[1,2]

[1]Medizinische Klinik und Poliklinik IV, Klinikum der Universität München, LMU München, München, Germany

[2]Division of Internal Medicine and Hypertension, Department of Medical Sciences, University of Turin, Turin, Italy

[3]Medizinische Klinik und Poliklinik IV, Diabetes Zentrum, Klinikum der Universität München, LMU München, München, Germany

[4]Institut für Prophylaxe und Epidemiologie der Kreislaufkrankheiten (IPEK), Klinikum der Universität München, München, Germany

[5]Division of Nephrology, University Hospital Carl Gustav Carus, Technische Universität Dresden, Dresden, Germany

[6]Klinik für Endokrinologie, Diabetologie und Klinische Ernährung, Universitätsspital Zürich, Zürich, Switzerland

Corresponding author:
Tracy Ann Williams, Medizinische Klinik und Poliklinik IV, Klinikum der Universität München, LMU München, Ziemssenstr. 1, D-80336 München, Germany
Tel: +49 89 4400 52941
Fax: +49 89 4400 54428
Email: Tracy.Williams@med.uni-muenchen.de; trwillia@unito.it

Total words: 3,000 + 4 figures + 2 tables

Online data supplement: Expanded methods, 4 figures and 4 tables

Running title: BEX1, ferroptosis and primary aldosteronism

Abstract

Aldosterone-producing adenomas (APA) are a major cause of primary aldosteronism. Somatic mutations in ion channels and transporters drive the aldosterone overproduction in the majority of APAs with mutations in the KCNJ5 G protein-coupled potassium channel predominating in most reported populations. Our objective was to gain insight into biological mechanisms of APA tumorigenesis by comparing transcriptomes of APAs of distinct sizes by mRNA sequencing analysis (9 APAs with adenoma diameter ≥30 mm *versus* 12 APAs ≤10 mm). Genes with significantly altered expression levels between these 2 groups were identified in APAs with no mutation detected (NMD, 348 genes) and with a *KCNJ5* mutation (155 genes). We validated the differential expression of 10 genes with a known function related to cell death and proliferation in an expanded sample set of 71 APAs by real-time qPCR (58 macro-APAs, diameter≥10 mm; 13 micro-APAs, diameter<10 mm). We focused on *BEX1* that was upregulated in micro-APAs relative to macro-APAs (2.76-fold, $P<0.001$) and compared with paired adrenal cortex (3.85-fold, $P<0.05$), and showed a linear negative correlation with APA diameter in the NMD group (r=-0.501, $P=0.007$). Compared with control cells, stable expression of BEX1 in human adrenocortical cells did not alter cell cycle progression or sensitivity to apoptosis but conferred protection from ferroptosis ($P<0.01$), a form of regulated cell death, measured by flow cytometry. Taken together, these findings demonstrate that BEX1 promotes cell survival in adrenal cells by mediating the inhibition of ferroptosis and suggest a function for *BEX1* in the pathogenesis of APAs.

Key words: aldosterone, cell death, primary aldosteronism, proliferation, regulated necrosis, tumorigenesis

Introduction

Primary aldosteronism (PA) is the most frequent surgically correctable cause of hypertension. The unilateral forms of the disease are mainly caused by an aldosterone-producing adenoma (APA) and are specifically treated and potentially cured by adrenalectomy.[1, 2] The surgically removed adrenals have been used to demonstrate the presence of somatic mutations in APAs in genes encoding ion channels (*KCNJ5*,[3] *CACNA1D,*[4, 5] *CACNA1H,*[6] *CLCN2*[7]) and transporters (*ATP1A1*,[5, 8] *ATP2B3*[8]). These mutations disturb ion homeostasis and activate Ca^{2+} signaling resulting in increased expression of *CYP11B2* (encoding aldosterone synthase) and constitutive aldosterone production.[6, 9] The use of targeted next-generation sequence analysis guided by CYP11B2-immunohistochemistry of paraffin-embedded adrenals has greatly increased the detection of somatic mutations in APAs to achieve a combined prevalence of over 90%.[10-12]

The role of the above mutations in cell death and proliferation is less clear. Activating somatic mutations in *CTNNB1*, encoding β-catenin, have been identified in APAs.[13] The prevalence of *CTNNB1* mutations in APAs is lower than in other adrenocortical tumors[14] but the proportion of APAs with constitutive Wnt/β-catenin signaling is high[15] implicating other factors in the activation of this pathway. Different *KCNJ5* mutations have diverse effects on adrenocortical cell growth[16] depending on the level of Na^+ conductance that determines the degree of cell toxicity.[3, 17]

We hypothesized that transcriptome profiling of APAs of distinctly different diameter may highlight genes that function in cell death and proliferation. We used mRNA sequencing (mRNA-seq) to compare the transcriptomes of small and large APAs from patients with PA

with a similar known duration of hypertension. Our objective was to identify novel genes and biological mechanisms involved in the deregulated cell growth of adrenal cells and translate these findings to a potential role in APA pathogenesis.

Materials and Methods

The authors declare that all supporting data are available within the article and its online supplementary files. mRNA-seq data have been made publicly available and can be accessed at https://github.com/MedIVLMUMunich/MacroMicroAPA_RNAseq

Patient samples

The study comprised 71 APAs surgically removed from patients diagnosed with unilateral PA at 2 referral centers (39 from the Medizinische Klinik IV, Klinikum der Ludwig-Maximilians-Universität München, Munich, Germany and 32 from the Hypertension unit, Department of Medical Sciences, University of Torino, Turin, Italy). For 17 APAs, the corresponding adjacent cortex was also available. PA was diagnosed according to current guidelines[1, 18] including adrenal venous sampling for subtype differentiation of unilateral from bilateral PA.[19] All patients included in the study displayed complete biochemical success after surgery according to the PASO criteria confirming the diagnosis of unilateral PA.[2, 20] The study also included 20 cortisol-producing adenomas and 8 incidentalomas diagnosed at the Munich center. Adenoma diameters were determined from the largest nodule at pathology. Research protocols were approved by local ethics committees, and all participants provided written informed consent.

Sanger sequencing of genomic DNA

KCNJ5 and hot spot regions of *ATP1A1*, *ATP2B3*, *CACNA1D* were sequenced by Sanger sequencing of PCR-amplified genomic DNA extracted from fresh frozen nodules resected from patients with APA as described previously,[21] *CTNNB1* was sequenced using primers shown in Table S1. The histopathology of all formalin-fixed paraffin embedded adrenals was evaluated using a specific CYP11B2 monoclonal antibody[22] to confirm the presence of an APA or an aldosterone-producing nodule in the resected gland.[23]

Next generation sequencing and bioinformatics analysis

mRNA-seq transcriptome profiling was performed of 21 APAs comprising 9 large macro-APAs with adenoma diameter ≥30 mm (5 with a *KCNJ5* mutation and 4 with NMD) and 12 micro-APAs with adenoma diameter ≤10 mm (6 with a *KCNJ5* mutation and 6 with NMD). mRNA-seq was performed by QIAGEN Genomics (Hilden, Germany). Heatmap and unsupervised hierarchical clustering and volcano plots were performed using R or the ClustVis web tool (https://biit.cs.ut.ee/clustvis/).[24]

Cell lines and culture conditions

Human adrenocortical (HAC15) cells[25] (a kind gift from Professor William E. Rainey, University of Michigan, Ann Arbor) were used to establish stable cell lines as described previously.[16]

Flow cytometry

Vibrant DyeCycle Violet stain was used for cell cycle analysis. Propidium iodide (PI) was used to quantify proportions of PI-positive dead cells following ferroptosis induction (with 4 µM [1*S*,3*R*]-RSL3 [RSL3]) in the presence or absence of ferroptosis inhibitor (10 µM liproxstatin-1,

[Lip-1]). Cell populations were detected on a FACSCalibur (BD Biosciences) or a BD Accuri C6 flow cytometer with FL2 detector (BD Biosciences). Data were analyzed with FLowJo version 10.4. All experiments were performed in triplicate, with a minimum of 7000 (cell cycle experiments) or 15000 (ferroptosis experiments) single cells analyzed per sample.

Statistical analysis

Statistical analyses were performed using IBM SPSS version 25.0 and GraphPad Prism version 8.2.1. Data were analyzed using the Kolmogorov-Smirnov test and Shapiro-Wilk test to determine distributions. Statistical significance was assessed by a t-test (paired where appropriate) or a Mann-Whitney test (Wilcoxon rank matched pairs test if needed) or a Bonferroni's post-test after two-way ANOVA. Chi-square and Fisher's exact tests were used to compare categorical variables. Univariate correlations were assessed using Pearson correlations. *P* values <0.05 were considered statistically significant.

Results

mRNA-Seq Transcriptome Analysis of APAs

Tumor samples used for mRNA-seq analysis (21 APAs) displayed a median nodule diameter of 34.0 mm [32.5-37.5] and 7.5 mm [6.3-10.0] (*P*<0.001), in each group (APAs ≥30 mm versus APAs ≤10 mm diameter). There were no significant differences between the 2 groups in known duration of hypertension (Table S2).

Unsupervised hierarchical clustering of 500 genes with the largest coefficient of variation classified four gene clusters categorized by genotype and adenoma diameter (Figure 1A). Differential expression analysis identified 348 and 155 significantly altered genes in the NMD

and *KCNJ5* subgroups, respectively (Figure 1B, 1C). Specifically, there were 119 upregulated and 229 downregulated DEGs in APAs with NMD, and 54 upregulated and 101 downregulated DEGs in the *KCNJ5* subgroup. The top 20 upregulated and downregulated genes in APAs (diameter ≥30 mm *versus* ≤10 mm) with NMD and with *KCNJ5* mutations are shown in Tables S3 and Table S4, respectively. The complete list of DEGs can be downloaded for: the total dataset: https://github.com/MedIVLMUMunich/MacroMicroAPA_RNAseq/raw/main/Total_DEGs.xlsx ; and stratified by APAs with NMD: https://github.com/MedIVLMUMunich/MacroMicroAPA_RNAseq/raw/main/NMD_DEGs.xlsx ; and with a *KCNJ5* mutation: https://github.com/MedIVLMUMunich/MacroMicroAPA_RNAseq/raw/main/KCNJ5_DEGs.xlsx

Gene Ontology Enrichment Analysis

DEGs were annotated to Gene Ontology (GO) terms of biological processes that identified different patterns of gene set enrichment between macro- and micro-APAs according to genotype (APAs with NMD and with a *KCNJ5* mutation). Cell death was the most significantly enriched biological process in APAs with NMD (P=6.4x10^{-8}) (Figure S1A). Other enriched GO terms in this group were related to axon guidance, angiogenesis, cell migration, the cellular response to zinc ions or Wnt signaling (Figure S1A). APAs with *KCNJ5* mutations showed enrichment of genes related to cholesterol biosynthesis, the cell cycle and cell division. Other enriched terms in this group were associated with RNA processing, signal transduction and organization of cellular components (Figure S1B).

DEGs Involved in Cell Death and Proliferation

Unsupervised hierarchical clustering of the top 40 DEGs associated with cell death and proliferation identified by the mRNA-seq analysis categorized gene clusters according to adenoma diameter in the NMD and *KCNJ5* subgroups (Figure S2). In the mRNA-seq analysis, no ferroptosis suppressor was differentially expressed in APAs with *KCNJ5* mutations. Conversely, 2 DEGs *MT1G* (metallothionein 1G) and *CAV1* (caveolin 1), encoding ferroptosis inhibitor proteins, were identified in the NMD subgroup ($\log_2$[APA ≥30 mm/ ≤10 mm]= 3.10, adjusted *P* value=0.0068; $\log_2$[APA ≥30 mm/ ≤10 mm]= -1.87, adjusted *P* value=0.0415) (Figure S3).

The expression levels of a subset of DEGs (identified by mRNA-seq analysis) with a reported role in cell death and proliferation, were determined in an expanded sample set of APAs (n=71; median diameter 15.0 mm [11.0-21.0]) (Table 1). APAs in this sample set were stratified into macro- and micro-APAs according to a cut-off diameter of 10 mm (macro-APAs [diameter ≥10 mm], n=58, median diameter, 16.0 mm [14.0-22.8]; micro-APAs [diameter <10 mm], n=13, median diameter, 7.0 mm [6.5-8.0], *P*<0.001). The macro-APA group comprised a higher proportion of women (63.8% and 30.8% in the macro- and micro-APA groups, respectively, *P*=0.029) and APAs with a *KCNJ5* mutation (67.2% in macro-APAs *versus* 30.8% in micro-APAs, *P*=0.015). The micro-APAs included a higher proportion of APAs with NMD (69.2% *versus* 32.8%) (Table 1).

Figure 1D shows the relative expression levels in macro- *versus* micro-APAs of 10 genes with a known role in cell death and proliferation. These genes included those with a role in β-catenin signaling (mRNA levels in macro- *versus* micro-APAs: *TSPAN12*, -8.30-fold, *P*<0.0001;

SFRP2, -5.85-fold, *P*<0.001; *DKK1*, -1.77-fold, *P*<0.01). *TSPAN12*, *BEX1*, *FBXL21*, and *TMPRSS3* gene expression levels were weakly correlated with adenoma diameter in the combined group of APAs (APAs with NMD+APAs with *KCNJ5* mutations), stronger correlations were observed in APAs with NMD (Table 2). In the NMD group, *FBXL21* and *TMPRSS3* gene expression was strongly positively correlated with adenoma diameter (*FBXL21*: r=0.761, *P*<0.001; *TMPRSS3*: r=0.727, *P*<0.001), a moderate negative correlation of *TSPAN12* and *BEX1* gene expression with adenoma diameter was observed (*TSPAN12*: r=-0.572, *P*=0.001; *BEX1*: r=-0.501, *P*=0.007) (Table 2).

BEX1 Gene Expression is Increased in Micro-APAs and Aldosterone-Producing Micronodules

In the expanded cohort of APAs (n=71), *BEX1* gene expression was 2.76-fold higher in micro-APAs relative to macro-APAs (*P*<0.001), and 2.31-fold upregulated in APAs with NMD compared with APAs with a *KCNJ5* mutation (*P*<0.0001) (Figure 2A, 2B). The linear negative correlation of *BEX1* gene expression with adenoma diameter in the NMD subgroup is shown in Figure 2C. Micro-APAs (n=5) displayed a 3.85-fold increase in *BEX1* expression compared with their paired adjacent cortex (*P*<0.05); whereas this difference was not observed for adrenals with macro-APAs (n=12) (Figure 2D). An analysis of *BEX1* mRNA levels in other adrenal tumors showed no apparent differences in *BEX1* gene expression according to tumor diameter in cortisol-producing adenomas (n=20) and in incidentalomas (n=8) (Figure 2E, 2F).

Analysis of publicly available transcriptome data[26] demonstrated significantly higher *BEX1* gene expression levels in aldosterone-producing micronodules (APMs, n=4), compared with paired zona fasciculata (zF, n=4; 8.75-fold, *P*<0.0001) and zona reticularis (n=4; 2.30-fold, *P*<0.05). In this small sample set, *BEX1* expression was higher, but did not reach statistical

significance, in APMs *versus* paired adjacent zona glomerulosa (zG, n=4; 1.87-fold, *P*=0.0501). Conversely, *BEX1* gene expression was significantly increased in zG relative to paired zF (4.69-fold, *P*<0.001) (Figure S4).

Role of BEX1 in Inhibition of Cell Death by Ferroptosis

We generated a stable human adrenocortical HAC15 cell line expressing BEX1 with a C-terminal DYKDDDDK tag (BEX1-DDK) (Figure 3A). Immunofluorescence staining demonstrated the localization of BEX1-DDK in the nucleus and cytoplasm (Figure 3B). The proportion of cells in the G0/G1, S and G2/M phases of the cell cycle was indistinguishable between HAC15 control and BEX1-DDK cells (Figure 3C, 3D). The effect of 2 μM staurosporine (STS)- an inducer of apoptosis- was highly similar in the BEX1-DDK cell line and HAC15 control cells in a cell viability assay (Figure 3E). In contrast, treatment with 4 μM RSL3 (a ferroptosis inducer) caused notably less cell death in the HAC15 BEX15-DDK cell line compared with HAC15 control cells (Figure 4A, 4B). The protective effect of BEX1 against RSL3-induced cell death, was confirmed by flow cytometry measurements using PI (propidium iodide) fluorescence staining of dead cells (Figure 4A, 4B, 4D). Specificity of RSL3-induced cell death was demonstrated by ablation of this response in the presence of 10 μM liproxstatin-1 (Lip-1, a ferroptosis inhibitor) (Figure 4C, 4D).

Discussion

We identified genes with significantly altered expression levels between APAs of distinct sizes with a focus on genes with a potential role in cell death and proliferation. We selected *BEX1*, encoding brain expressed X-linked 1,[27] for further study because the function of this gene in the adrenal cortex is unknown and differential expression levels of *BEX1* in different subsets

of APAs have been previously reported.[5] Using in vitro functional analyses employing flow cytometry of human adrenocortical cell lines with stable overexpression of BEX1, we demonstrated a novel role for BEX1 as a suppressor of cell death by ferroptosis.

BEX1 transcripts are abundantly expressed in brain. In peripheral tissues, the highest gene expression levels are observed in the adrenal and testis.[27, 28] Previous studies have reported a role for BEX1 in the regeneration of neurons,[29] skeletal muscle[30] and liver,[31] associated with its function in cell cycle regulation[29] and apoptosis.[31] In addition, BEX1 has been identified as a part of a ribonucleoprotein processing complex that promotes translocation and maturation of mRNAs encoding pro-inflammatory genes in the heart.[32]

Ferroptosis is an iron-dependent form of regulated cell death, morphologically and biochemically distinct from apoptosis, characterized by the accumulation of redox-active iron, lipid hydroperoxides, and oxidized polyunsaturated fatty acid-containing phospholipids.[33-35] Adrenocortical cells are especially sensitive to ferroptosis,[36, 37] an observation likely related to the vulnerability of steroidogenic tissues to redox imbalance caused by electron leakage by cytochrome P450 enzymes and reactive oxygen species generation.[38-41]

Herein, we report an inverse correlation of *BEX1* gene expression with APA diameter and an upregulation of *BEX1* transcription in micro-APAs, but not macro-APAs, compared with paired adjacent adrenal cortex. The differential expression levels of *BEX1* in different adrenal tissue samples may reflect different levels of steroidogenesis and production of reactive oxygen species. In this context, *BEX1*-mediated protection from ferroptosis may involve a response to increased steroidogenesis and oxidative stress thereby providing a growth advantage for zona

glomerulosa cells with aldosterone overproduction over adjacent cells. Thus, these findings may translate to a role for *BEX1* in APA pathogenesis via promoting cell survival and facilitating adenoma formation. In support of this concept, analysis of publicly available transcriptome data[26] revealed relatively high *BEX1* gene expression in APMs (the revised nomenclature for aldosterone-producing cell clusters),[23] a potential origin of APAs,[42, 43] compared with paired adrenocortical zones.

Like APMs, micro-APAs display strong CYP11B2 (aldosterone synthase) immunostaining.[23, 26, 44] In micro-APAs, CYP11B2 immunoreactivity per tumor area is more intense than in macro-APAs[44] and the intensity of CYP11B2 immunostaining is inversely correlated with APA diameter.[44, 45] The higher CYP11B2 expression associated with micro-APAs is likely required for sufficient aldosterone production to cause clinically overt PA from small adenomas.[44] In support of this, in the present study, the baseline median plasma aldosterone concentration of the micro-APA group was similar to that of the macro-APA group, indicating the microadenomas could sustain high levels of steroidogenesis despite their smaller size.

If CYP11B2 immunoreactivity is taken as a surrogate of pathological steroidogenesis associated with an APA, decreased CYP11B2 immunoreactivity per tumor area with increasing APA diameter may suggest a reduced ability to elicit an oxidative stress response.[39, 41, 46] Thus there would be a decreased requirement for anti-ferroptotic mechanisms and *BEX1* gene expression. The protection from a cell death mechanism in tumors of a small size may appear paradoxical, but we have previously reported that APAs with NMD (unlike in APAs with a *KCNJ5* mutation) display a decreased proliferation index with increasing adenoma diameter[16] indicating a progressive activation of anti-proliferation mechanisms. Taken together,

mechanisms that control different forms of cell death and proliferation likely initiate and self-regulate tumor growth to restrict the size of a subset of APAs.

In a microarray analysis of 8 APAs with *KCNJ5* mutations compared with 5 APAs with *CACNA1D* or *ATP1A1* mutations, Azizan et al,[5] identified *BEX1* as a differentially expressed gene with significantly increased expression in adenomas with *CACNA1D* or *ATP1A1* mutations. Because these tumors tend to be small, with diameters less than 10 mm,[5] our findings of increased *BEX1* transcription in micro-APAs are in agreement with the report of Azizan et al.[5] However, it is unclear if the high *BEX1* expression and modulation of ferroptosis in the NMD group we detected is related to APAs of small diameter in general or to a specific aldosterone-driver mutation or mutations which we were unable to detect by our sequencing approach. In a later study,[47] and of high relevance to the present work, the same group of researchers, identified a role for oxidative stress in APA pathogenesis by the analysis of the transcriptomes of APAs with their paired zona glomerulosa.[47] The study demonstrated that the top canonical biological pathway associated with the differentially expressed genes (APA versus paired zona glomerulosa) was the NRF2 (nuclear factor erythroid 2–related factor 2)-mediated oxidative stress response[47] which is a critical cellular mechanism to maintain intracellular redox homeostasis and limit oxidative damage.[48]

A strength of our study is the transcriptome analysis using sample stratification by adenoma diameter and genotype to specifically identify genes that function in cell death and proliferation. An additional strength is the validation of gene expression levels in a large sample cohort from two expert referral centers using standardized diagnostic procedures.[49] Furthermore, all APAs used in the study were resected from patients with complete

biochemical success after surgery highlighting the appropriate diagnosis of unilateral PA.[2] Finally, we performed a functional characterization of the *BEX1* gene to identify a novel role in adrenocortical cells which is relevant to APA pathogenesis. The sequencing approach we used is a study limitation as it was not targeted to CYP11B2-positive lesions and therefore the NMD group potentially contained aldosterone-driver mutations.[10-12]

In conclusion, the *BEX1* gene is differentially expressed in APAs according to nodule diameter and protects human adrenocortical cells in vitro from a form of regulated cell death called ferroptosis.

Perspectives

Ferroptosis, a form of cell death associated with cell metabolism and redox biology, may function in the pathogenesis of APAs. Future studies are required to clarify this function and elucidate the potential role of BEX1. We are currently planning further transcriptomics studies using our stable BEX1 adrenocortical cell lines and flow cytometry analyses of single cell suspensions, isolated from APA and paired adjacent cortex tissue samples, treated with ferroptosis inducers and inhibitors to gain a better understanding of the role of BEX1 and of ferroptosis in adrenocortical cells.

Acknowledgements

The excellent support of Elisabeth Christine Obster from the German Conn registry is gratefully acknowledged and the expert technical assistance of Isabella-Sabrina Kinker and Petra Rank.

Sources of Funding

This work was financed by the Deutsche Forschungsgemeinschaft (DFG) project number 444776998 to T.A. Williams (WI 5359/2-1) and M. Reincke (RE 752/31-1) and project number 314061271-TRR 205/project B15 to T.A. Williams (within the CRC/Transregio 205/1 "The Adrenal: Central Relay in Health and Disease"). The CRC/Transregio 205/1 also supports the work of C. Adolf, F. Beuschlein, and M. Reincke. This study was also supported by the European Research Council under the European Union Horizon 2020 research and innovation program (grant agreement No. 694913 to M. Reincke) and the Else Kröner-Fresenius Stiftung in support of the German Conn's Registry-Else-Kröner Hyperaldosteronism Registry (2013_A182, 2015_A171 and 2019_A104 to M. Reincke). Y. Yang is in receipt of a Ph.D. fellowship from the China Scholarship Council.

Conflicts of interest/ Disclosures

None

References

1. Funder JW, Carey RM, Mantero F, Murad MH, Reincke M, Shibata H, Stowasser M, Young WF, Jr. The management of primary aldosteronism: case detection, diagnosis, and treatment: an endocrine society clinical practice guideline. *J Clin Endocrinol Metab*. 2016;101:1889-1916. doi: 10.1210/jc.2015-4061
2. Williams TA, Lenders JWM, Mulatero P, Burrello J, Rottenkolber M, Adolf C, Satoh F, Amar L, Quinkler M, Deinum J, et al. Outcomes after adrenalectomy for unilateral primary aldosteronism: an international consensus on outcome measures and analysis of remission rates in an international cohort. *Lancet Diabetes Endocrinol*. 2017;5:689-699. doi: 10.1016/S2213-8587(17)30135-3
3. Choi M, Scholl UI, Yue P, Björklund P, Zhao B, Nelson-Williams C, Ji W, Cho Y, Patel A, Men CJ, et al. K+ channel mutations in adrenal aldosterone-producing adenomas and hereditary hypertension. *Science*. 2011;331:768-772. doi: 10.1126/science.1198785
4. Scholl UI, Goh G, Stölting G, de Oliveira RC, Choi M, Overton JD, Fonseca AL, Korah R, Starker LF, Kunstman JW, et al. Somatic and germline CACNA1D calcium channel mutations in aldosterone-producing adenomas and primary aldosteronism. *Nat Genet*. 2013;45:1050-1054. doi: 10.1038/ng.2695
5. Azizan EA, Poulsen H, Tuluc P, Zhou J, Clausen MV, Lieb A, Maniero C, Garg S, Bochukova EG, Zhao W, et al. Somatic mutations in ATP1A1 and CACNA1D underlie a common subtype of adrenal hypertension. *Nat Genet*. 2013;45:1055-1060. doi: 10.1038/ng.2716
6. Nanba K, Blinder AR, Rege J, Hattangady NG, Else T, Liu CJ, Tomlins SA, Vats P, Kumar-Sinha C, Giordano TJ, Rainey WE. Somatic CACNA1H mutation as a cause of

aldosterone-producing adenoma. *Hypertension*. 2020;75:645-649. doi: 10.1161/HYPERTENSIONAHA.119.14349

7. Dutta RK, Arnesen T, Heie A, Walz M, Alesina P, Söderkvist P, Gimm O. A somatic mutation in CLCN2 identified in a sporadic aldosterone-producing adenoma. *Eur J Endocrinol*. 2019;181:K37-K41. doi: 10.1530/EJE-19-0377
8. Beuschlein F, Boulkroun S, Osswald A, Wieland T, Nielsen HN, Lichtenauer UD, Penton D, Schack VR, Amar L, Fischer E, et al. Somatic mutations in ATP1A1 and ATP2B3 lead to aldosterone-producing adenomas and secondary hypertension. *Nat Genet*. 2013;45:440-444, 444e1-444e2. doi: 10.1038/ng.2550
9. Oki K, Plonczynski MW, Luis Lam M, Gomez-Sanchez EP, Gomez-Sanchez CE. Potassium channel mutant KCNJ5 T158A expression in HAC-15 cells increases aldosterone synthesis. *Endocrinology*. 2012;153:1774-1782. doi: 10.1210/en.2011-1733
10. Nanba K, Omata K, Else T, Beck PCC, Nanba AT, Turcu AF, Miller BS, Giordano TJ, Tomlins SA, Rainey WE. Targeted molecular characterization of aldosterone-producing adenomas in white americans. *J Clin Endocrinol Metab*. 2018;103:3869-3876. doi: 10.1210/jc.2018-01004
11. De Sousa K, Boulkroun S, Baron S, Nanba K, Wack M, Rainey WE, Rocha A, Giscos-Douriez I, Meatchi T, Amar L, Travers S, Fernandes-Rosa FL, Zennaro MC. Genetic, cellular, and molecular heterogeneity in adrenals with aldosterone-producing adenoma. *Hypertension*. 2020;75:1034-1044. doi: 10.1161/HYPERTENSIONAHA.119.14177
12. Nanba K, Yamazaki Y, Bick N, Onodera K, Tezuka Y, Omata K, Ono Y, Blinder AR, Tomlins SA, Rainey WE, Satoh F, Sasano H. Prevalence of somatic mutations in

aldosterone-producing adenomas in japanese patients. *J Clin Endocrinol Metab*. 2020;105:dagg595. doi: 10.1210/clinem/dgaa595

13. Åkerström T, Maharjan R, Sven Willenberg H, Cupisti K, Ip J, Moser A, Stålberg P, Robinson B, Alexander Iwen K, Dralle H, et al. Activating mutations in CTNNB1 in aldosterone producing adenomas. *Sci Rep*. 2016;6:19546. doi: 10.1038/srep19546

14. Tissier F, Cavard C, Groussin L, Perlemoine K, Fumey G, Hagneré AM, René-Corail F, Jullian E, Gicquel C, Bertagna X, Vacher-Lavenu MC, Perret C, Bertherat J. Mutations of beta-catenin in adrenocortical tumors: activation of the Wnt signaling pathway is a frequent event in both benign and malignant adrenocortical tumors. *Cancer Res*. 2005;65:7622-7627. doi: 10.1158/0008-5472.CAN-05-0593

15. Berthon A, Drelon C, Ragazzon B, Boulkroun S, Tissier F, Amar L, Samson-Couterie B, Zennaro MC, Plouin PF, Skah S, et al. Wnt/β-catenin signalling is activated in aldosterone-producing adenomas and controls aldosterone production. *Hum Mol Genet*. 2014;23:889-905. doi: 10.1093/hmg/ddt484

16. Yang Y, Gomez-Sanchez CE, Jaquin D, Aristizabal Prada ET, Meyer LS, Knösel T, Schneider H, Beuschlein F, Reincke M, Williams TA. Primary aldosteronism: KCNJ5 mutations and adrenocortical cell growth. *Hypertension*. 2019;74:809-816. doi: 10.1161/HYPERTENSIONAHA.119.13476

17. Scholl UI, Nelson-Williams C, Yue P, Grekin R, Wyatt RJ, Dillon MJ, Couch R, Hammer LK, Harley FL, Farhi A, Wang WH, Lifton RP. Hypertension with or without adrenal hyperplasia due to different inherited mutations in the potassium channel KCNJ5. *Proc Natl Acad Sci U S A*. 2012;109:2533-2538. doi: 10.1073/pnas.1121407109

18. Mulatero P, Monticone S, Deinum J, Amar L, Prejbisz A, Zennaro MC, Beuschlein F, Rossi GP, Nishikawa T, Morganti A, Seccia TM, Lin YH, Fallo F, Widimsky J. Genetics,

prevalence, screening and confirmation of primary aldosteronism: a position statement and consensus of the working group on endocrine hypertension of the european society of hypertension. *J Hypertens*. 2020;38:1919-1928. doi: 10.1097/HJH.0000000000002510

19. Mulatero P, Sechi LA, Williams TA, Lenders JWM, Reincke M, Satoh F, Januszewicz A, Naruse M, Doumas M, Veglio F, Wu VC, Widimsky J. Subtype diagnosis, treatment, complications and outcomes of primary aldosteronism and future direction of research: a position statement and consensus of the working group on endocrine hypertension of the european society of hypertension. *J Hypertens*. 2020;38:1929-1936. doi: 10.1097/HJH.0000000000002520

20. Yang Y, Reincke M, Williams TA. Treatment of unilateral PA by adrenalectomy: potential reasons for incomplete biochemical cure. *Exp Clin Endocrinol Diabetes*. 2019;127:100-108. doi: 10.1055/a-0662-6081

21. Yang Y, Burrello J, Burrello A, Eisenhofer G, Peitzsch M, Tetti M, Knösel T, Beuschlein F, Lenders JWM, Mulatero P, Reincke M, Williams TA. Classification of microadenomas in patients with primary aldosteronism by steroid profiling. *J Steroid Biochem Mol Biol*. 2019;189:274-282. doi: 10.1016/j.jsbmb.2019.01.008

22. Gomez-Sanchez CE, Qi X, Velarde-Miranda C, Plonczynski MW, Parker CR, Rainey W, Satoh F, Maekawa T, Nakamura Y, Sasano H, Gomez-Sanchez EP. Development of monoclonal antibodies against human CYP11B1 and CYP11B2. *Mol Cell Endocrinol*. 2014;383:111-117. doi: 10.1016/j.mce.2013.11.022

23. Williams TA, Gomez-Sanchez CE, Rainey WE, Giordano TJ, Lam AK, Marker A, Mete O, Yamazaki Y, Zerbini MCN, Beuschlein F, et al. International histopathology consensus

for unilateral primary aldosteronism. *J Clin Endocrinol Metab*. 2021;106:42-54. doi: 10.1210/clinem/dgaa484

24. Metsalu T, Vilo J. Clustvis: a web tool for visualizing clustering of multivariate data using principal component analysis and heatmap. *Nucleic Acids Res*. 2015;43:W566-570. doi: 10.1093/nar/gkv468

25. Parmar J, Key RE, Rainey WE. Development of an adrenocorticotropin-responsive human adrenocortical carcinoma cell line. *J Clin Endocrinol Metab*. 2008;93:4542-4546. doi: 10.1210/jc.2008-0903

26. Nishimoto K, Tomlins SA, Kuick R, Cani AK, Giordano TJ, Hovelson DH, Liu CJ, Sanjanwala AR, Edwards MA, Gomez-Sanchez CE, Nanba K, Rainey WE. Aldosterone-stimulating somatic gene mutations are common in normal adrenal glands. *Proc Natl Acad Sci U S A*. 2015;112:E4591-4599. doi: 10.1073/pnas.1505529112

27. Yang QS, Xia F, Gu SH, Yuan HL, Chen JZ, Yang QS, Ying K, Xie Y, Mao YM. Cloning and expression pattern of a spermatogenesis-related gene, BEX1, mapped to chromosome Xq22. *Biochem Genet*. 2002;40:1-12. doi: 10.1023/a:1014565320998

28. Fagerberg L, Hallström BM, Oksvold P, Kampf C, Djureinovic D, Odeberg J, Habuka M, Tahmasebpoor S, Danielsson A, Edlund K, et al. Analysis of the human tissue-specific expression by genome-wide integration of transcriptomics and antibody-based proteomics. *Mol Cell Proteomics*. 2014;13:397-406. doi: 10.1074/mcp.M113.035600

29. Vilar M, Murillo-Carretero M, Mira H, Magnusson K, Besset V, Ibáñez CF. Bex1, a novel interactor of the p75 neurotrophin receptor, links neurotrophin signaling to the cell cycle. *EMBO J*. 2006;25:1219-1230. doi: 10.1038/sj.emboj.7601017

30. Jiang C, Wang JH, Yue F, Kuang S. The brain expressed x-linked gene 1 (Bex1) regulates myoblast fusion. *Dev Biol*. 2016;409:16-25. doi: 10.1016/j.ydbio.2015.11.007

31. Gu Y, Wei W, Cheng Y, Wan B, Ding X, Wang H, Zhang Y, Jin M. A pivotal role of BEX1 in liver progenitor cell expansion in mice. *Stem Cell Res Ther*. 2018;9:164. doi: 10.1186/s13287-018-0905-2

32. Accornero F, Schips TG, Petrosino JM, Gu SQ, Kanisicak O, van Berlo JH, Molkentin JD. BEX1 is an RNA-dependent mediator of cardiomyopathy. *Nat Commun*. 2017;8:1875. doi: 10.1038/s41467-017-02005-1

33. Dixon SJ, Lemberg KM, Lamprecht MR, Skouta R, Zaitsev EM, Gleason CE, Patel DN, Bauer AJ, Cantley AM, Yang WS, Morrison B 3rd, Stockwell BR. Ferroptosis: an iron-dependent form of nonapoptotic cell death. *Cell*. 2012;149:1060-1072. doi: 10.1016/j.cell.2012.03.042

34. Stockwell BR, Friedmann Angeli JP, Bayir H, Bush AI, Conrad M, Dixon SJ, Fulda S, Gascón S, Hatzios SK, Kagan VE, et al. Ferroptosis: a regulated cell death nexus linking metabolism, redox biology, and disease. *Cell*. 2017;171:273-285. doi: 10.1016/j.cell.2017.09.021

35. Dixon SJ, Stockwell BR. The hallmarks of ferroptosis. *Annu Rev Cancer Biol*. 2019;3:35–54. doi: 10.1146/annurev-cancerbio-030518-055844

36. Belavgeni A, Bornstein SR, von Mässenhausen A, Tonnus W, Stumpf J, Meyer C, Othmar E, Latk M, Kanczkowski W, Kroiss M, et al. Exquisite sensitivity of adrenocortical carcinomas to induction of ferroptosis. *Proc Natl Acad Sci U S A*. 2019;116:22269-22274. doi: 10.1073/pnas.1912700116

37. Weigand I, Schreiner J, Röhrig F, Sun N, Landwehr LS, Urlaub H, Kendl S, Kiseljak-Vassiliades K, Wierman ME, Angeli JPF, Walch A, Sbiera S, Fassnacht M, Kroiss M. Active steroid hormone synthesis renders adrenocortical cells highly susceptible to type II ferroptosis induction. *Cell Death Dis*. 2020;11:192. doi: 10.1038/s41419-020-2385-4

38. Rapoport R, Sklan D, Hanukoglu I. Electron leakage from the adrenal cortex mitochondrial P450scc and P450c11 systems: NADPH and steroid dependence. *Arch Biochem Biophys*. 1995;317:412-416. doi: 10.1006/abbi.1995.1182

39. Prasad R, Kowalczyk JC, Meimaridou E, Storr HL, Metherell LA. Oxidative stress and adrenocortical insufficiency. *J Endocrinol*. 2014;221:R63-R73. doi: 10.1530/JOE-13-0346

40. Lim JB, Barker KA, Eller KA, Jiang L, Molina V, Saifee JF, Sikes HD. Insights into electron leakage in the reaction cycle of cytochrome P450 BM3 revealed by kinetic modeling and mutagenesis. *Protein Sci*. 2015;24:1874-1883. doi: 10.1002/pro.2793

41. Zou Y, Li H, Graham ET, Deik AA, Eaton JK, Wang W, Sandoval-Gomez G, Clish CB, Doench JG, Schreiber SL. Cytochrome P450 oxidoreductase contributes to phospholipid peroxidation in ferroptosis. *Nat Chem Biol*. 2020;16:302-309. doi: 10.1038/s41589-020-0472-6

42. Nishimoto K, Seki T, Kurihara I, Yokota K, Omura M, Nishikawa T, Shibata H, Kosaka T, Oya M, Suematsu M, Mukai K. Case report: nodule development from subcapsular aldosterone-producing cell clusters causes hyperaldosteronism. *J Clin Endocrinol Metab*. 2016;101:6-9. doi: 10.1210/jc.2015-3285

43. Sun N, Meyer LS, Feuchtinger A, Kunzke T, Knösel T, Reincke M, Walch A, Williams TA. Mass spectrometry imaging establishes 2 distinct metabolic phenotypes of

aldosterone-producing cell clusters in primary aldosteronism. *Hypertension*. 2020;75:634-644. doi: 10.1161/HYPERTENSIONAHA.119.14041

44. Ono Y, Nakamura Y, Maekawa T, Felizola SJ, Morimoto R, Iwakura Y, Kudo M, Seiji K, Takase K, Arai Y, Gomez-Sanchez CE, Ito S, Sasano H, Satoh F. Different expression of 11β-hydroxylase and aldosterone synthase between aldosterone-producing microadenomas and macroadenomas. *Hypertension*. 2014;64:438-444. doi: 10.1161/HYPERTENSIONAHA.113.02944

45. Monticone S, Castellano I, Versace K, Lucatello B, Veglio F, Gomez-Sanchez CE, Williams TA, Mulatero P. Immunohistochemical, genetic and clinical characterization of sporadic aldosterone-producing adenomas. *Mol Cell Endocrinol*. 2015;411:146-154. doi: 10.1016/j.mce.2015.04.022

46. Shimada K, Hayano M, Pagano NC, Stockwell BR. Cell-line selectivity improves the predictive power of pharmacogenomic analyses and helps identify NADPH as biomarker for ferroptosis sensitivity. *Cell Chem Biol*. 2016;23:225-235. doi: 10.1016/j.chembiol.2015.11.016

47. Zhou J, Lam B, Neogi SG, Yeo GS, Azizan EA, Brown MJ. Transcriptome pathway analysis of pathological and physiological aldosterone-producing human tissues. *Hypertension*. 2016;68:1424-1431. doi: 10.1161/HYPERTENSIONAHA.116.08033

48. Ma Q. Role of nrf2 in oxidative stress and toxicity. *Annu Rev Pharmacol Toxicol*. 2013;53:401-426. doi: 10.1146/annurev-pharmtox-011112-140320

49. Williams TA, Reincke M. Management of endocrine disease: diagnosis and management of primary aldosteronism: the endocrine society guideline 2016 revisited. *Eur J Endocrinol*. 2018;179:R19-R29. doi: 10.1530/EJE-17-0990

Novelty and Significance

What is New?

- Transcriptome profiles of aldosterone-producing adenomas with highly diverse diameters are distinctly different
- Gene ontology enrichment analysis identifies over-representation of cell death in a subset of aldosterone-producing adenomas
- The *BEX1* (brain expressed X-linked 1) gene is upregulated in micro- compared with macro-aldosterone-producing adenomas and with paired adjacent adrenal cortex
- In human adrenocortical cells in vitro, BEX1 confers protection from ferroptosis- a form of nonapoptotic regulated cell death

What is relevant?

- mRNA-seq analysis of aldosterone-producing adenomas of diverse sizes identifies a multitude of genes involved in cell growth mechanisms
- BEX1 may promote cell survival in small aldosterone-producing adenomas by mediating the inhibition of ferroptosis

Summary

BEX1 suppresses ferroptosis in human adrenocortical cells and may play a role in the pathogenesis of aldosterone-producing adenomas.

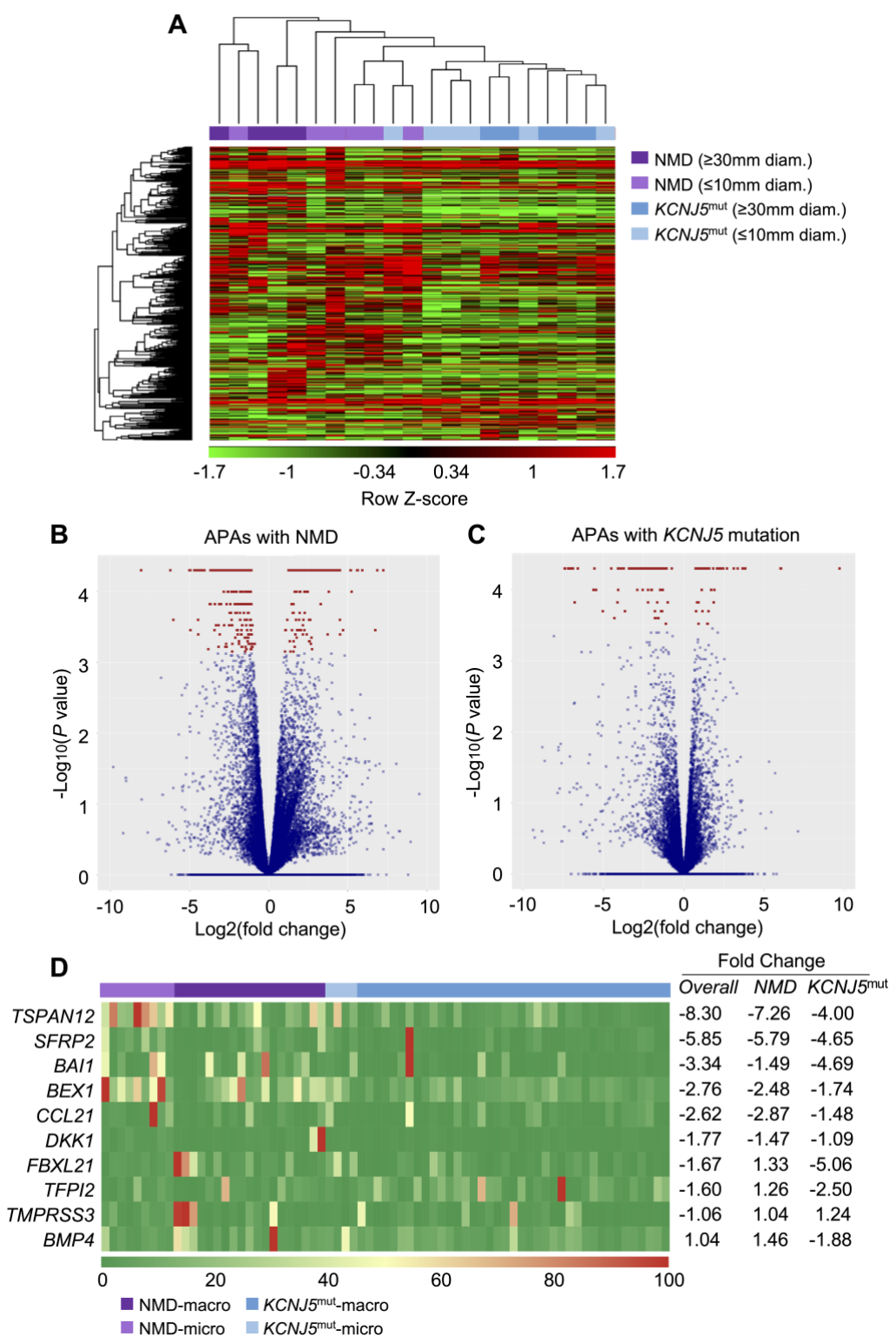

Figure 1. Distinct transcriptome profiles in APAs with different genotypes and adenoma diameters.

The heat map shows unsupervised hierarchical clustering of 500 genes with the largest coefficient of variation based on normalized FPKM (fragments per kilobase of transcript, per million mapped reads) identified by mRNA-seq (**A**). Row Z-score indicates the difference in expression level of a gene in standard deviation units from the mean expression level in all

samples. Volcano plots by mRNA-seq analysis highlight genes in red that were differentially expressed in APAs with NMD (**B**) or with a *KCNJ5* mutation (**C**). Differential expression was defined as an adjusted *P* value <0.05 using the Benjamini-Hochberg False Discovery Rate method. Red dots in the region of Log_2(fold change) <0 represent downregulated genes in APAs ≥30mm diameter compared with ≤10mm diameter; red dots in the region of Log_2(fold change) >0 represents upregulated genes in the NMD and *KCNJ5*^{mut} subgroups as indicated. The second heatmap shows the mRNA expression levels of 10 genes, determined by real-time qPCR, of an expanded cohort of 71 APAs. The 10 genes selected for study were all DEGs of interest identified from the mRNA-seq analysis with a previously described role in cell death and proliferation (**D**). Genes studied are shown on the left of the figure, sample identity is color-coded at the top of the figure, and fold changes in gene expression (real-time qPCR quantification) are shown on the right, in the overall group (NMD+*KCNJ5*^{mut}) and stratified for APAs with NMD or *KCNJ5* mutations (*KCNJ5*^{mut}). The color-coded matrix shows the relative quantification (RQ) values of genes for each sample ($2^{-\Delta\Delta Ct}$) compared with the median micro-APA gene expression level of each gene. RQ values were then transformed to a 0 to 100 grading scale with the smallest RQ value set as 0 and largest value as 100. Macro-APAs are defined as ≥10 mm; micro-APAs as <10mm diameter. APAs, aldosterone-producing adenomas; diam., diameter; *KCNJ5*, gene encoding potassium inwardly rectifying channel subfamily J member 5; *KCNJ5*^{mut}, APAs with *KCNJ5* mutations; NMD, APAs with no mutation detected.

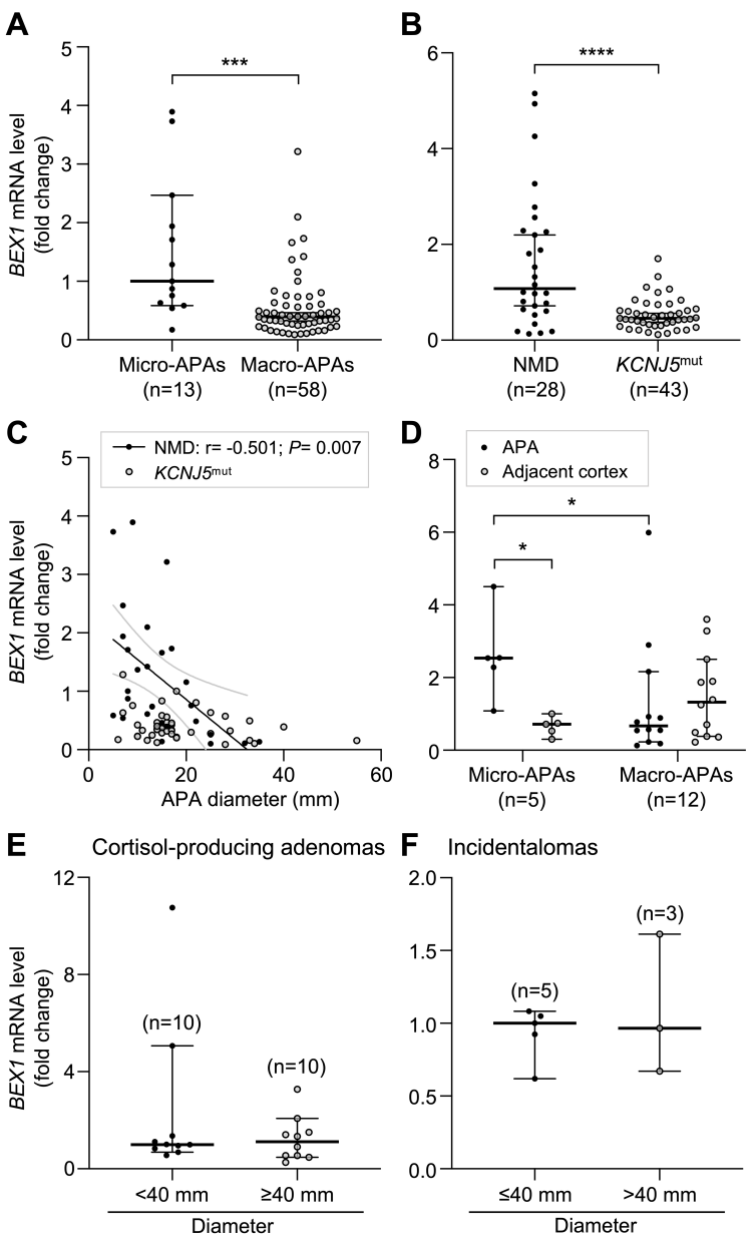

Figure 2. *BEX1* gene expression in adrenal tumors.

Real time qPCR analysis of *BEX1* gene expression in micro and macro-APAs (**A**) and in APAs with NMD and with a *KCNJ5*-mutation (**B**). A linear negative correlation of *BEX1* gene expression was observed with APA diameter in APAs with NMD (**C**). *BEX1* gene expression was higher in micro-APAs compared with their paired adjacent cortex but not in macro-APAs relative to paired adjacent adrenal cortex (**D**). There were no apparent differences in *BEX1* gene expression according to adenoma size in cortisol-producing adenomas (**E**) and incidentalomas (**F**). Statistical analyses were performed on $2^{-\Delta\Delta Ct}$ values using a Mann-Whitney test, Pearson correlation analysis or a Wilcoxon matched-pairs signed rank test. **P*<0.05, ****P*<0.001, *****P*<0.0001. Each point represents a single sample. Horizontal lines indicate the median, whiskers represent 95% confidential intervals. APA, aldosterone-producing adenoma; *KCNJ5*, gene encoding potassium inwardly rectifying channel subfamily J member 5; *KCNJ5*^{mut}, APAs with *KCNJ5* mutations; n, number; NMD, APAs with no mutation detected.

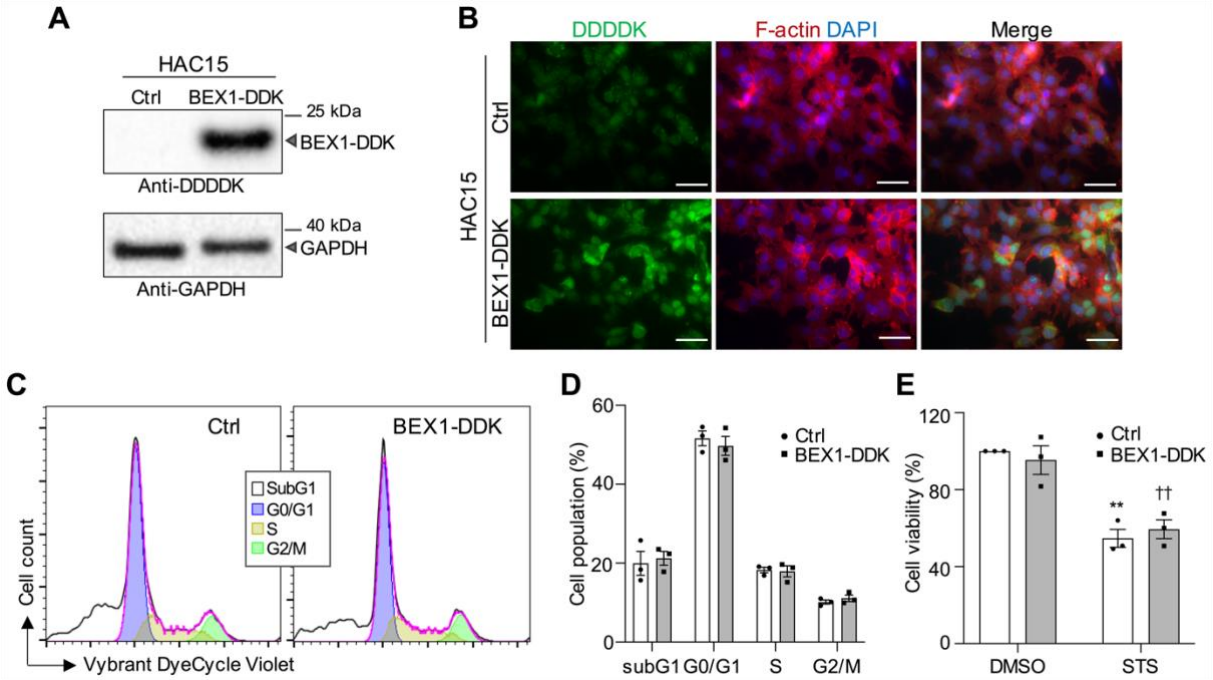

Figure 3. BEX1 has no effect on cell cycle progression and apoptosis in adrenocortical cells. Western blot analysis of HAC15 cells selected for stable expression of empty vector (HAC15 Ctrl) or BEX1 with a C-terminal DYKDDDDK tag (BEX1-DDK) (**A**). Anti-DDDDK immunofluorescence staining of BEX1-DDK expressed in HAC15 cells compared with HAC15 Ctrl cells with F-actin and DAPI stain highlighting the cytoplasm and nucleus, respectively (**B**). HAC15 cell cycle analysis of Ctrl and BEX1-DDK cells, measured by flow cytometry with Vybrant DyeCycle violet DNA staining in a representative experiment (**C**) and from 3 independent experiments (**D**). Cell viability of HAC15 Ctrl and BEX1-DDK cells after 6 hours treatment with vehicle (0.02% DMSO) or 2 µM STS (staurosporine, inducer of apoptosis). Data are normalized to the HAC15 Ctrl cell line treated with 0.02% DMSO vehicle and data are shown from 3 independent experiments (**E**). In panel **E**, **difference (P<0.01) from HAC15 Ctrl cells treated with vehicle, ††difference (P<0.01) from HAC15 BEX1-DDK cells treated with vehicle. BEX1-DDK, HAC15 cells with stable expression of BEX1 with a C-terminal DYKDDDDK tag; Ctrl, HAC15 cells with stable expression of empty vector; DAPI, 4', 6-diamidino-2-phenylindole, dihydrochloride; DDK, DDDDK tag; DMSO, dimethyl sulfoxide; F-actin, filamentous actin; GAPDH, glyceraldehyde 3-phosphate dehydrogenase; STS, staurosporine. Scale bar=50 µm.

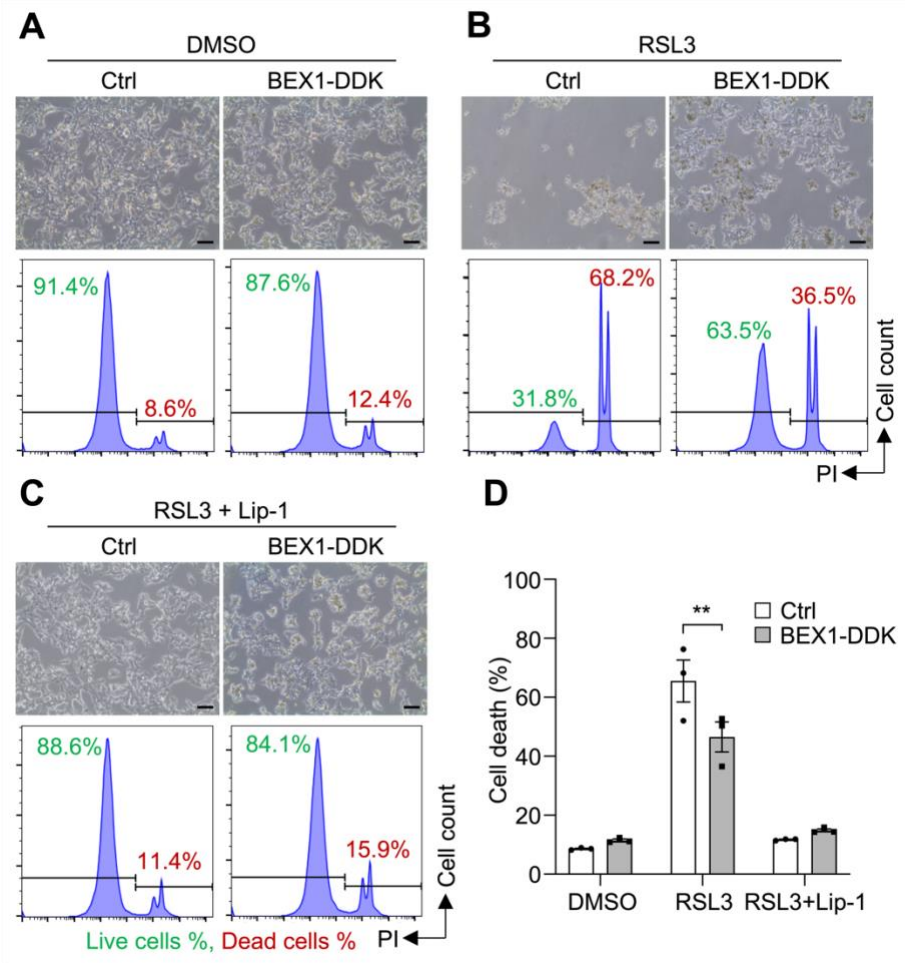

Figure 4. BEX1 inhibits cell death by ferroptosis in adrenocortical cells.

HAC15 BEX1-DDK cells are less susceptible to cell death caused by the ferroptosis inducer RSL3 ([1*S*,3*R*]-RSL3) compared with the HAC15 Ctrl cell line **(upper panels of A, B)**. Analysis of cell death by flow cytometry with PI (propidium iodide) of HAC15 Ctrl and BEX1-DDK cells after treatment with vehicle (0.004% DMSO), 4 µM RSL3 or 4 µM RSL3 + 10 µM Lip-1 for 24 hours. The proportion (%) of PI-negative cells (alive, in green) or positive cells (dead, in red) measured by flow cytometry is indicated within each chromatogram in a representative experiment **(lower panels of A, B, C)** and from 3 independent experiments (**D**). Bars represent means of three independent experiments, error bars indicate SEM. *P* values were calculated by two-way ANOVA with a Bonferroni's post-test. In panel **D**, **difference ($P<0.01$) between HAC15 BEX1-DDK cells and HAC15 Ctrl cells treated with RSL3. BEX1-DDK, HAC15 cells with stable expression of BEX1 with a C-terminal DYKDDDDK tag; Ctrl, HAC15 cells with stable expression of empty vector; DDK, DDDDK tag; DMSO, dimethyl sulfoxide; Lip-1, liproxstatin-1; PI, propidium iodide; RSL3, (1*S*,3*R*)-RSL-3.

Variables	Total cohort (n=71)	Macro-APA (n=58)	Micro-APA (n=13)	*P* value
Age at surgery (years; n=71)	48.2 ± 11.5	48.2 ± 11.4	48.1 ± 12.4	0.978
Sex (ref. women; n=71)	41 (57.7%)	37 (63.8%)	4 (30.8%)	0.029
BMI (kg/m^2; n=66)	26.2 [22.7-30.1]	26.0 [22.4-30.0]	26.4 [23.4-31.5]	0.502
Systolic BP (mmHg; n=68)	150 [140-166]	149 [140-161]	160 [150-174]	0.029
Diastolic BP (mmHg; n=68)	94 [85-101]	92 [85-100]	100 [88-108]	0.217
Duration HTN (months; n=69)	97 [29-171]	99 [24-174]	97 [51-207]	0.586
Anti-HTN meds (DDD; n=66)	3.0 [1.5-4.8]	3.0 [1.1-4.5]	3.7 [2.6-4.9]	0.179
PAC (pmol/L; n=69)	838 [590-1419]	859 [586-1404]	805 [571-1523]	0.939
DRC (mU/L; n=36)	3.4 [2.0-7.6]	3.3 [2.0-8.2]	4.5 [2.4-6.5]	0.903
ARR_DRC (n=36)	197 [92-356]	218 [92-371]	160 [89-283]	0.480
PRA (pmol/L/min; n=32)	2.6 [2.3-6.4]	2.6 [2.6-5.1]	6.4 [1.3-8.3]	0.564
ARR_PRA (n=32)	352 [142-596]	377 [150-609]	225 [111-841]	0.458
Lowest serum K^+ (mmol/L; n=70)	3.0 ± 0.6	2.9 ± 0.6	3.2 ± 0.4	0.145
Nodule diam. (mm; n=71)	15.0 [11.0-21.0]	16.0 [14.0-22.8]	7.0 [6.5-8.0]	< 0.001
APAs_*KCNJ5* mutation (n=43)	43 (60.6%)	39 (67.2%)	4 (30.8%)	0.015
APAs_NMD (n=28)	28 (39.4%)	19 (32.8%)	9 (69.2%)	0.015
Clinical outcome (n=63)				0.115
Complete success	27 (42.9%)	25 (47.2%)	2 (20.0%)	
Partial success	28 (44.4%)	23 (43.4%)	5 (50.0%)	
Absent success	8 (12.7%)	5 (9.4%)	3 (30.0%)	
Biochemical outcome (n=61)				NA

Complete success	61 (100.0%)	50 (100.0%)	11 (100.0%)
Partial success	0 (0.0%)	0 (0.0%)	0 (0.0%)
Absent success	0 (0.0%)	0 (0.0%)	0 (0.0%)

Table 1. **Clinical and biochemical parameters of patients with APA stratified by adenoma diameter.**

All variables refer to baseline data. Nodule diam. refers to the diameter of the largest adrenal nodule at pathology. Macro-APAs were defined by diameter of the largest nodule ≥10 mm; micro-APAs were defined by diameter of the largest nodule <10 mm. Quantitative normally distributed variables are expressed as means ±SD and quantitative non-normally distributed variables are reported as medians [IQR]. Categorical variables are presented as absolute numbers and percentages. *P* values were calculated using Chi-square and Fisher's exact tests or t test or Mann-Whitney test as appropriate. *P* values of less than 0.05 were considered significant. APA, aldosterone-producing adenoma; ARR, aldosterone-to-renin ratio; BMI, body mass index; BP, blood pressure; DDD, defined daily dose; diam., diameter; DRC, direct renin concentration; HTN, hypertension; K^+, potassium ions; *KCNJ5*, gene encoding potassium inwardly rectifying channel subfamily J member 5; meds, medications; n, number; NA, not applicable; NMD, no mutation detected; PAC, plasma aldosterone concentration; PRA, plasma renin activity; ref., reference. The defined daily dose is the assumed average maintenance dose per day for a drug used for its main indication in adults according to ATC/DDD Index 2019 https://www.whocc.no/atc_ddd_index/.

Gene	Protein	Overall		NMD		*KCNJ5*^{mut}	
		r	*P*	r	*P*	r	*P*
TSPAN12	Tetraspanin 12	-0.388	0.001	-0.572	0.001	-0.148	0.344
SFRP2	Secreted frizzled-related protein 2	-0.038	0.760	-0.397	0.036	0.129	0.433
BAI1	Brain-specific angiogenesis inhibitor 1	-0.105	0.411	-0.210	0.293	0.068	0.689
BEX1	Brain expressed X-linked 1	-0.376	0.001	-0.501	0.007	-0.241	0.119
CCL21	Chemokine, C-C motif, ligand 21	-0.152	0.207	-0.249	0.201	-0.037	0.813
DKK1	Dickkopf-related protein 1	-0.139	0.249	-0.169	0.390	-0.175	0.269
FBXL21	F-box and leucine rich repeat protein 21	0.361	0.005	0.761	< 0.001	-0.251	0.159
TFPI2	Tissue factor pathway inhibitor 2	0.039	0.748	0.017	0.932	0.008	0.959
TMPRSS3	Transmembrane serine protease 3	0.443	0.001	0.727	< 0.001	0.317	0.083
BMP4	Bone morphogenetic protein 4	0.111	0.358	0.389	0.041	-0.124	0.427

Table 2. Correlation of gene expression levels with APA diameter according to genotype.

Values indicate Pearson correlation coefficients (r) and respective *P* values in the overall group (NMD+*KCNJ5*^{mut}) of APAs or stratified for APAs with NMD or *KCNJ5* mutations. Gene expression levels of 71 APAs (28 with NMD and 43 with *KCNJ5* mutations) were determined

by real-time qPCR as described in the online supplemental methods section. *KCNJ5*, gene encoding potassium inwardly rectifying channel subfamily J member 5; *KCNJ5*^{mut}, *KCNJ5* gene mutations; NMD, no mutation detected.